UPS Operation of Multi-Terminal Smart Transformer for Islanded Operation of Data Centres

Dwijasish Das
Student Member, IEEE
Dept. of EEE, IIT Guwahati
Guwahati, India
dwijasish@iitg.ac.in

Anandh N
Student Member, IEEE
Dept. of EEE, IIT Guwahati
Guwahati, India
anandh_n@iitg.ac.in

Chandan Kumar
Senior Member, IEEE
Dept. of EEE, IIT Guwahati
Guwahati, India
chandank@iitg.ac.in

2022 IEEE International Conference on Power Electronics, Drives and Energy Systems (PEDES) | 978-1-6654-5566-4/22/$31.00 ©2022 IEEE | DOI: 10.1109/PEDES56012.2022.10080692

***Abstract*—With the ever-growing demand of internet-based services globally, the power demand and energy consumption in data centres are consistently rising. To enhance the efficiency of the power conversion stages from the medium voltage (MV) utility grid to the low voltage (LV) level in data centres, smart transformer (ST) provides a prominent solution. Thereby, significantly decreasing the number of cascaded power conversion stages, ensuing lesser complexity, high reliability, high power density/efficiency o f d ata c entre p ower s upplies. I n t his paper, a multi-terminal (MT) ST is proposed for data centres, and particularly its uninterrupted power supply (UPS) mode of operation for continuity of power supply is explored. The MTST is an extension of the ST by replacing the dual-active bridge in the isolation stage with a multi-active bridge. This allows the ST to have multiple LVdc ports which are utilized for server loads in the data centres and also to exchange power from renewable sources/energy storage systems. The MTST can also be operated as an UPS at times of power outages. The simulation of the proposed system is done in PSCAD software to verify its operation in UPS mode, ensuring uninterrupted power to the data centres.**

***Index Terms*—data centres, LVdc system, multi-terminal smart transformer, UPS operation**

I. Introduction

Data centres play significant r ole i n p rocessing massive data-sets and initializing online services including search, video streaming, and scientific computing. Due to the development of internet of things (IoT), cloud computing, and mobile internet, there is a rapid increase of energy consumption in data centres [1]. The persistent blooming of internet/cloud services signify that data centres are the major energy consumers in future. The major power-hungry devices in data centres are the servers. These servers are considered to be the key computational loads that operate at low dc voltage. Subsequently, conversion of power is necessary from high voltage ac utility grid to the low voltage dc loads [2]. The chain of power supply of the data centres from the medium voltage (MV) utility grid to the low-level voltage comprises of several cascaded power conversion stages, as a result it shows comparatively low efficiency. To enhance the efficiency by considerably reducing the stages of power conversion and directly interconnecting the MVac grid to low voltage (LV) ac and dc buses, smart transformer (ST) is an emerging candidate [3]–[5]. Being a power electronic transformer, the ST interfaces the medium voltage (MV) grid and the LV load. It is the main power conversion element which incorporates energy sources and loads into the grids offering several features like high efficiency, high power density, low electromagnetic interference (EMI), high reliability, reasonable cost, etc. [6]. Furthermore, it offers a promising solution in data centres for better power flow management with high flexibility and providing dc grid connectivity [7]. Based on control and communication architectures the ST performs the function of energy router, such that it manages, optimizes and regulates the power flow connecting the grid and data centre [8], [9].

The uninterrupted power supply (UPS) system is a back-up/alternative source of power, connecting the main power supply and the loads. It offers back-up power and protects the sensitive loads from line frequency variations [10]. Requirement of UPS operation is very essential in a data centre whenever there is a fault occurrence in the grid or for maintenance. Major challenges during the UPS operation are detection, isolation and synchronization at the time of reconnection to the grid [11]. To overcome these problems, various schemes on detection/protection are discussed in the literature to make sure that distributed generation (DG) systems can be operated as uninterruptible power supply when detached from the utility grid [12].

Whenever the power is absorbed or injected in the feeders, it should be balanced for all the operational modes. Specifically, grid supplying mode is most challenging on both ac terminals. This demands the absorption of necessary power from dc links, either from dc grids or energy storage devices [13]. The incorporation of energy storage devices with the dc ports is a possible solution to enable the UPS mode of operation for a short time duration. Moreover, because of the limited generation and capacity, it is compulsory to control both the generation and load. To attain this, both the ac and dc grid voltages have to be controlled [14].

The UPS operation of a three stage multi-terminal (MT) smart transformer for power delivery in data centres is presented in this paper. The arms of the MTST are designed such that it meets the voltage requirements of a typical data centre.

This publication is supported by the Intel India Research Fellowship Program 2021-22, under the project entitled “Smart Transformer Enabled Hybrid Grid for Efficient and Green Data Centres”.

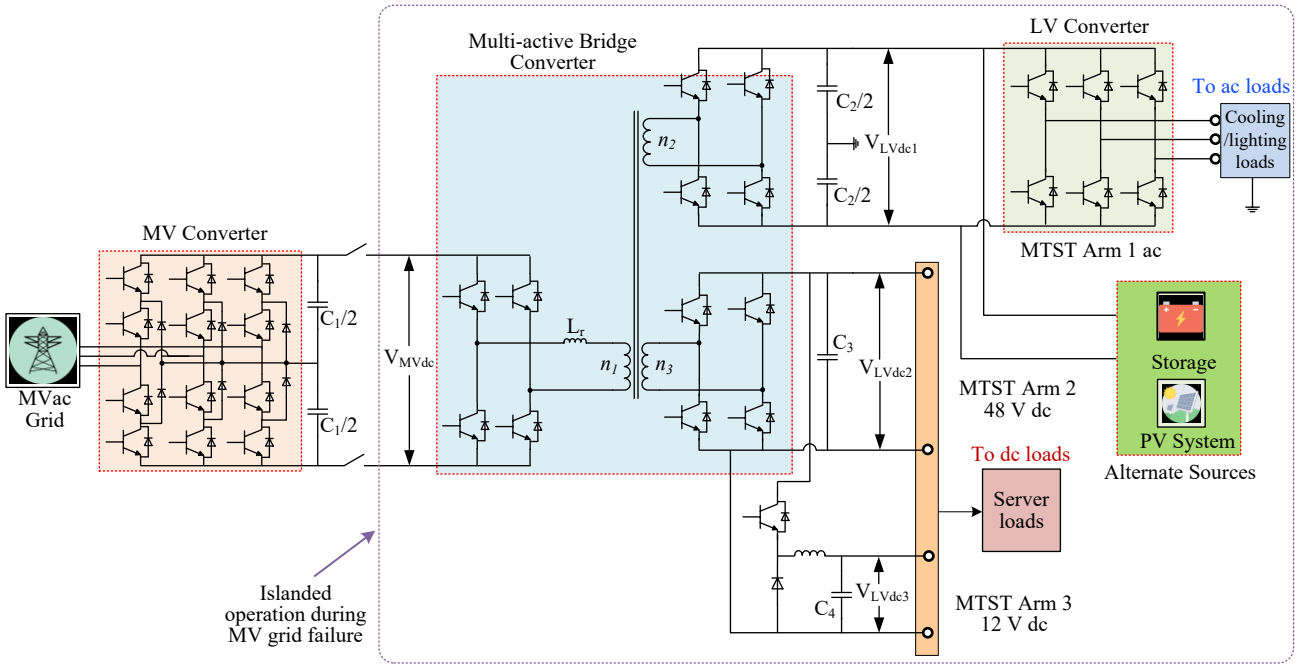

Fig. 1. Schematic diagram of the MTST feeding power to a data centre.

The paper is structured as follows. Section II elaborates the proposed MTST, Section III explains the power management during UPS operation of MTST, Section IV presents the control strategies for the MTST converters and Section V shows the simulation results. Lastly, Section VI concludes the paper.

II. Description of the Proposed System

The schematic diagram of the MTST feeding power to a data centre is shown in Fig. 1. The MTST MV converter takes power from the MVac grid and converts it to MVdc. The MTST multi-active bridge (MAB) converter in the next stage converts the MVdc into two different LVdc levels - 1 kV and 48 V. A buck converter is used to provide another terminal of 12 V from the 48 V LVdc bus. The 1 kV LVdc bus is interfaced to the third stage of the MTST i.e. LV converter, which converts the power to LVac for the ac loads in the data centre like lighting and cooling. Moreover, the 1 kV LVdc bus is also utilized to interface a PV system as well as a battery energy storage system (BESS). The BESS is employed to store the excess PV power and also for the UPS operation of the MTST during utility grid power outages. The 48 V and 12 V supplies are directly given to the server loads.

III. Proposed Power Management Scheme During Islanded Operation

During the proposed islanded operation of the system, the MTST MV converter is turned OFF. The MVdc side of the MAB is also not functional. The power is fed from the BESS system interfaced to the 1 kV LVdc bridge of the MAB. The available PV power is also fed from the PV system to the same 1 kV bus. From this bus, the MTST LV converter draws power to supply the LVac loads of the data centre. The 48 V LVdc bridge also draws power from the 1 kV LVdc bridge through the multi-winding high frequency isolation transformer. In the islanded mode, the sources are the PV and BESS. Therefore, the power supplied by the BESS is given by

$$P_{BESS} = P_{LVac} + P_{LVdc1} + P_{LVdc2} + P_{LVdc3} - P_{pv} \quad (1)$$

where P_{LVac} is the power drawn by the LVac load of the data centre. P_{LVdc1}, P_{LVdc2} and P_{LVdc3} are the power drawn by the loads at the 1 kV, 48 V and 12 V LVdc buses, respectively and P_{pv} is the power injected by the PV system.

In the islanded operation, the MV side is disconnected. The power flows from the 1 kV LVdc bridge to the 48 V LVdc bridge of the MAB through the high frequency isolation transformer and is expressed as

$$P_{2-3} = \frac{V_{LVdc1} V_{LVdc2}}{2\pi\ f_s L_{2-3}} \phi_{2-3} \left(1 - \frac{|\phi_{2-3}|}{\pi}\right) \quad (2)$$

where V_{LVdc1} and V_{LVdc2} are the dc link voltages of the bridges 2 and 3. f_s is the switching frequency, L_{2-3} is the leakage inductance between bridges 2 and 3 and ϕ_{2-3} is the firing angle delay between bridges 2 and 3.

In (2), P_{2-3} is also the total power drawn by the 48 V and 12 V LVdc loads. Thus

$$P_{2-3} = P_{LVdc2} + P_{LVdc3}. \quad (3)$$

Therefore, (1) can be written as

$$P_{BESS} = P_{LVac} + P_{LVdc1} + P_{2-3} - P_{pv}. \quad (4)$$

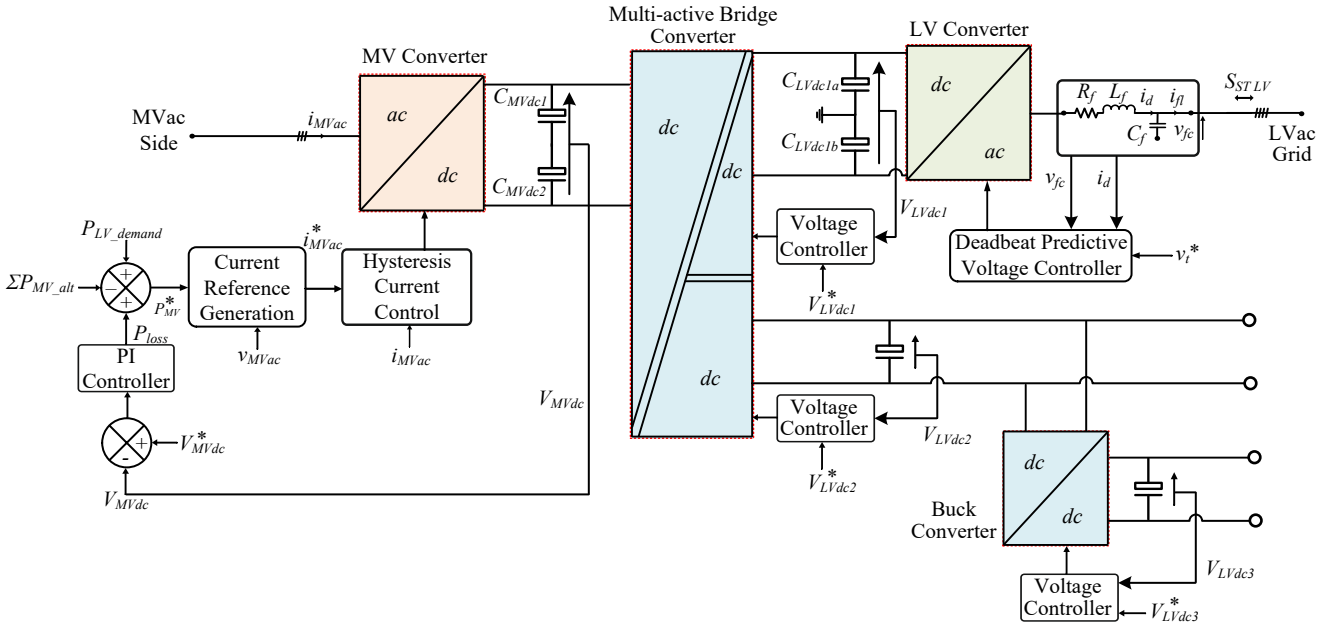

Fig. 2. Overall control diagram.

IV. Control Strategies

Fig. 2 depicts the overall control diagram. The control strategies consist of controlling the MV converter, the MAB to maintain the 1 kV and 48 V LVdc bus voltage, a dc-dc buck converter to control the 12 V LVdc bus, the MTST LV converter to maintain the LVac voltage and the BESS dc-dc converter. These are discussed as follows.

A. MV Converter

This converter is operational during the grid connected mode. It draws the power requirement of the data centre loads from the MVac side. Reference currents are generated from instantaneous symmetric component theory [15] and a hysteresis controller is utilized to regulate the actual currents as per reference. In the islanded mode when the UPS operation starts, this converter is not functional.

B. MAB Converter

This is a triple-active bridge converter and maintains 1 kV and 48 V LVdc bus voltages by drawing power from the 20 kV MVdc bus, in the grid connected mode. During the islanded mode of operation, the converter acts as a dual-active bridge as the MVdc bridge is turned off. The 1 kV LVdc bridge acts as the primary and the 48 V LVdc bridge acts as the secondary. Power is drawn by this converter from the 1 kV LVdc bus to maintain the 48 V LVdc bus. This enables the loads to draw the required power from the 48 V bus. Both the bridges are fired with square waves of 50% duty ratio. The delay between the square waves of the primary and secondary side bridges determines the power flow. The delay is controlled with a proportional integral (PI) controller to maintain the 48 V dc bus. It is expressed as follows.

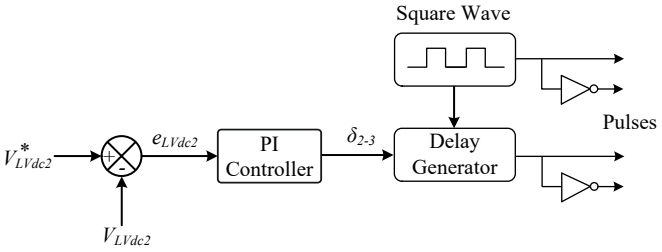

Fig. 3. Control diagram of the MAB converter in UPS mode.

$$\delta_{2-3} = K_{pm} e_m + K_{im} \int e_m \, dt \tag{5}$$

where K_{pm} and K_{im} are the proportional and integral gains of the MAB converter for the power flow from 1 kV LVdc bridge to the 48 V bridge. e_m is the error between the reference and actual LVdc voltage. Fig. 3 shows the control diagram of the MAB converter in the UPS mode of operation.

C. LV Converter

The LV converter regulates the LVac voltage and frequency which is mainly utilized by the lighting and cooling loads of the data centre. A dead-beat control strategy is utilized to maintain the LVac voltage and frequency based on the reference [16]. An LC filter is used for filtering the voltage and to obtain sinusoidal output. The state space representation of the LC filter dynamics is given by $\dot{\mathbf{x}} = \mathbf{A}\mathbf{x} + \mathbf{B}\mathbf{z}$, where $\mathbf{A} = \begin{bmatrix} 0 & \frac{1}{C_f} \\ \frac{1}{L_f} & -\frac{R_f}{L_f} \end{bmatrix}$, $\mathbf{B} = \begin{bmatrix} 0 & \frac{1}{C_f} \\ \frac{V_{LVdc1}}{L_f} & 0 \end{bmatrix}$, $\mathbf{x} = [v_{fc} \quad i_d]^T$ and $\mathbf{z} = [u_c \quad i_{fl}]^T$. v_{fc}, i_d, and i_{fl} are voltage of the capacitor,

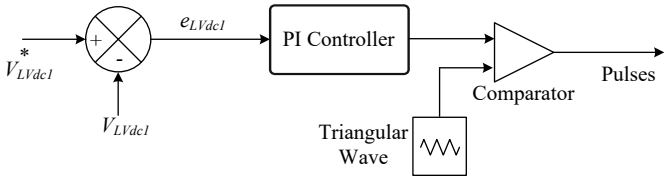

Fig. 4. Control diagram of the BESS converter in UPS mode.

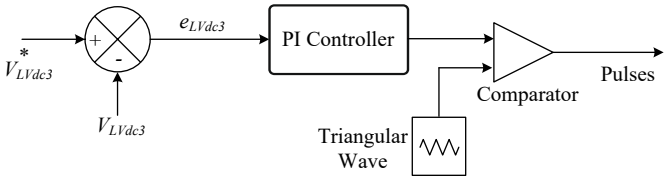

Fig. 5. Control diagram of the dc-dc buck converter.

current of the inductor and output filter, respectively. u_c is a switching control variable with value $+V_{LVdc1}$ or $-V_{LVdc1}$. The state space equation can be converted to discrete time domain with a sampling instant of k. Thus, v_{fc} at the $(k+1)^{th}$ instant is derived as:

$$v_{fc}(k+1) = G_{11}v_{fc}(k) + G_{12}i_d(k) + H_{11}u_c(k) + H_{12}i_{fl}(k) \tag{6}$$

where $\mathbf{G} = e^{\mathbf{A}T_d}$, $\mathbf{H} = \int_0^{T_d} e^{\mathbf{A}t}\mathbf{B}dt$ and T_d is the sampling time.

A cost function is taken as $J = \{v_{fc}(k+1) - v_t^*(k+1)\}^2$ and it is minimized by differentiating and considering it equal to zero. This gives:

$$v_{fc}(k+1) = v_t^*(k+1). \tag{7}$$

Using equations (6) and (7), a control law is generated as follows:

$$u_c^*(k) = \frac{v_t^*(k+1) - G_{11}v_{fc}(k) - G_{12}i_{fl}(k) - H_{12}i_d(k)}{H_{11}}. \tag{8}$$

A hysteresis controller is utilized to maintain $u_c^*(k)$ and accordingly switching pulses are generated for the MTST LV converter.

D. BESS Converter

The BESS converter operates in current control mode in the grid connected mode of operation. When UPS operation is necessary, it switches to voltage control mode and maintains the 1 kV LVdc bus voltage. A PI controller is employed to regulate the actual voltage around the reference voltage. The control diagram of the BESS converter in UPS mode is shown in Fig. 4.

E. 12 V dc-dc Buck Converter

A buck dc-dc converter is used to step down the 48 V LVdc to 12 V. The converter operates to maintain the constant voltage of 12 V and this is implemented with another PI controller. The actual voltage is compared with the reference of 48 V and the error is sent to the PI controller. The PI controller output is correlated with a triangular wave to generate the firing pulses for the converter. The control diagram of the dc-dc buck converter is depicted in Fig. 5.

V. Simulation Results

The simulation of the proposed system is done in PSCAD software to verify the UPS operation. The system parameters are given in Table I.

TABLE I
Simulation Parameters

System quantities	Values
MV grid voltage	11 kV (L-L)
LV grid voltage	0.4 kV (L-L)
MTST MV converter	Power Rating = 100 kVA, L_{fm} = 100 mH, C_{fm} = 1 μF C_{MVdc} = 1350 μF
MTST MAB converter	No of windings = 3, f_s = 2 kHz, V_{MVdc} = 20 kV, V_{LVdc1} = 1 kV, V_{LVdc2} = 48 V
MTST LV converter	Power Rating = 100 kVA, C_{LVdc} = 4700 μF, L_f = 1 mH, C_f = 20 μF
12 V dc-dc buck converter	Power Rating = 2 kW, f_{sw} = 10 kHz C_{LVdc3} = 83 μF, L_{12} = 1 mH

Fig. 6(a) depicts the power taken from the MVac side. Fig. 6(b)-(f) depicts the LVac load, 48 V dc load, 12 V dc load, PV power and BESS power, respectively. Initially, the LVac, LVdc2 and LVdc3 loads are 50 kW, 10 kW and 1 kW, respectively. The PV system injects a power of 10 kW at the LVdc bus 1. In the grid connected mode, the balance power requirement is taken from the MVac side and BESS does not supply any power. At t = 0.5 s, the MVac grid fails and the BESS starts supplying the balance power while maintaining the 1 kV LVdc bus voltage. All the ac and dc loads keep drawing the same amount of power as before. At t = 0.7 s, the LVac load increases to 60 kW. This increase in load is supplied by the BESS and remaining power are left undisturbed. At t = 0.9 s, the LVdc2 load increases from 10 kW to 12 kW. The increased load is again reflected on the power supplied by the BESS. At t = 1.1 s, the LVdc3 load increases from 1 kW to 1.5 kW and a corresponding increase is seen on the power drawn from the BESS. The remaining system is undisturbed. At t = 1.3 s, the PV power injection increases from 10 kW to 15 kW. This results in the decrease in power drawn from the BESS and the remaining powers are not affected.

Fig. 7 exhibits the ac currents and voltages in the system during the change over from grid connected to islanded mode (UPS operation). Fig. 7(a) shows the MVac currents. These become zero as the MVac side is disconnected. Fig. 7(b) and (c) shows the LVac voltage and current, respectively. These remain undisturbed during the transition.

Fig. 8 shows the ac currents and voltages in the system during ac load change in UPS mode of operation. The increased LVac load is observed in the LVac currents. The LVac voltage is not disturbed.

The dc bus voltage in the system are shown in Fig. 9. The MVdc bus voltage is shown in Fig. 9(a). Initially, this is maintained at 20 kV. After t = 0.5 s, the MVdc bus voltage is not controlled by any converter. As there is no discharge

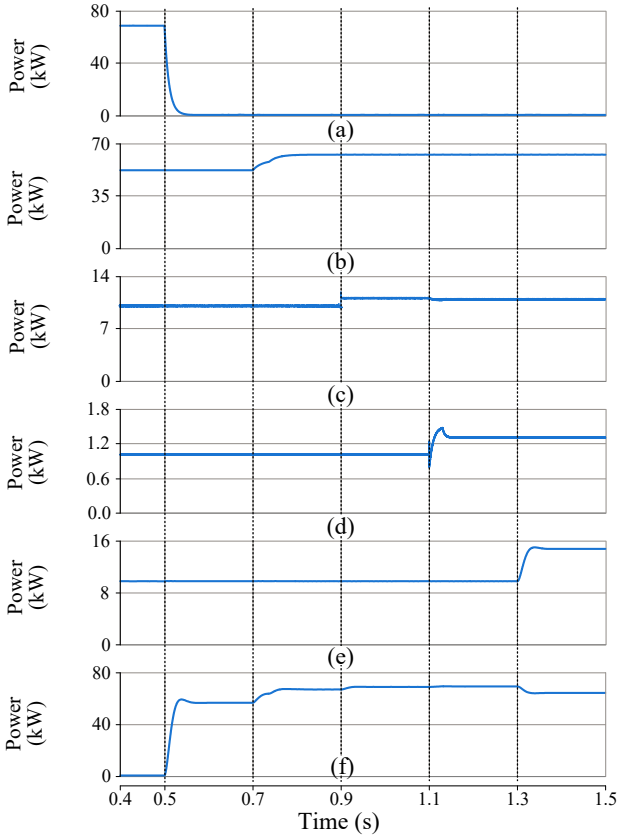

Fig. 6. Power flows in the system. (a) Power drawn from MVac side. (b) LVac load. (c) 48 V dc load. (d) 12 V dc load. (e) PV power. (f) BESS power.

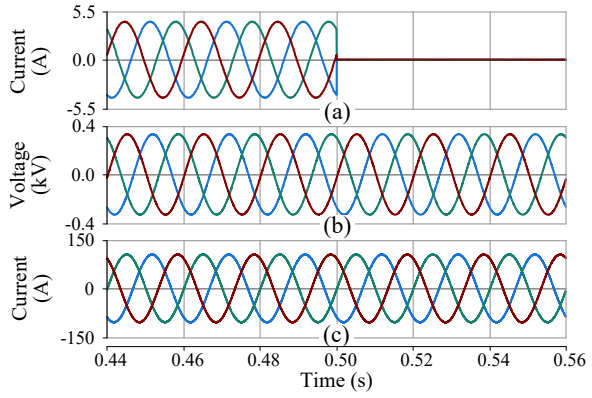

Fig. 7. Ac voltages and currents in the system during transition to UPS mode of operation. (a) MVac current. (b) LVac voltage. (c) LVac current.

path for the MVdc capacitor voltage, the voltage remains constant. Fig. 9(b)-(d) shows the LVdc1, LVdc2 and LVdc3 bus voltages, respectively. These are maintained at 1 kV, 48 V and 12 V, respectively and negligible disturbance is seen when the UPS operation starts. Moreover, the system operates smoothly throughout the load changes at the different buses. This verifies the UPS operation of the MTST.

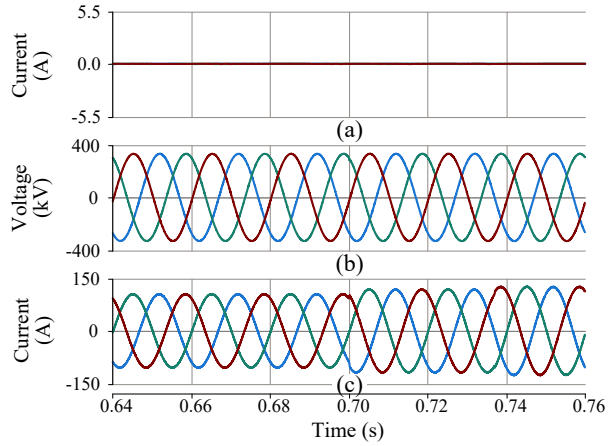

Fig. 8. Ac voltages and currents in the system for ac load change during UPS operation. (a) MVac current. (b) LVac voltage. (c) LVac current.

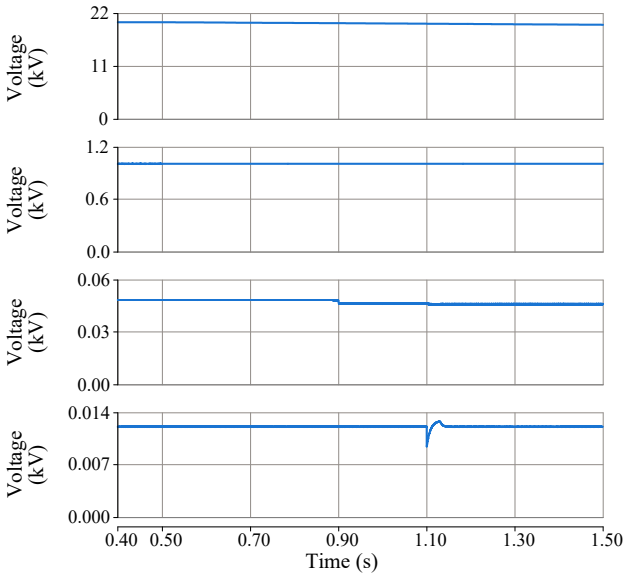

Fig. 9. Dc bus voltages in the system. (a) MVdc voltage. (b) LVdc1 voltage. (c) LVdc2 voltage. (d) LVdc3 voltage.

VI. Conclusions

The UPS operation of a three stage multi-terminal (MT) smart transformer for power delivery in data centres has been proposed in this paper. Such a system provides uninterrupted power to a data centre at times of utility power outages. The UPS operation remains as an alternative source of power whenever power outages occur. This operation ensures the reliability of the data centre. A BESS system is linked to the 1 kV LVdc bus of the MTST and it acts as backup power. During UPS operation, the multi-active bridge (MAB) of the MTST is partially operated to transfer power from the 1 kV bridge to the 48 V bridge, while keeping the MVdc bridge turned OFF. The proposed scheme enables smooth transfer from grid connected operation to UPS operation without the need of additional components. Moreover, it can facilitate load

changes at the different load buses along with variation in PV power injection. Simulation results have been furnished validating the proposed operation.

REFERENCES

[1] K. M. U. Ahmed, M. H. J. Bollen, and M. Alvarez, "A review of data centers energy consumption and reliability modeling," *IEEE Access*, vol. 9, pp. 152 536–152 563, 2021.

[2] B. R. Shrestha, U. Tamrakar, T. M. Hansen, B. P. Bhattarai, S. James, and R. Tonkoski, "Efficiency and reliability analyses of ac and 380 v dc distribution in data centers," *IEEE Access*, vol. 6, pp. 63 305–63 315, 2018.

[3] M. Liserre, G. Buticchi, M. Andresen, G. De Carne, L. F. Costa, and Z.-X. Zou, "The smart transformer: Impact on the electric grid and technology challenges," *IEEE Ind. Electron. Mag.*, vol. 10, no. 2, pp. 46–58, 2016.

[4] L. Ferreira Costa, G. De Carne, G. Buticchi, and M. Liserre, "The smart transformer: A solid-state transformer tailored to provide ancillary services to the distribution grid," *IEEE Power Electron. Mag.*, vol. 4, no. 2, pp. 56–67, 2017.

[5] D. Das, V. M. Hrishikesan, C. Kumar, and M. Liserre, "Smart transformer-enabled meshed hybrid distribution grid," *IEEE Trans. Ind. Electron.*, vol. 68, no. 1, pp. 282–292, 2021.

[6] L. Zheng, R. P. Kandula, and D. Divan, "Soft-switching solid-state transformer with reduced conduction loss," *IEEE Trans. Power Electron.*, vol. 36, no. 5, pp. 5236–5249, 2021.

[7] X. She, A. Q. Huang, and R. Burgos, "Review of solid-state transformer technologies and their application in power distribution systems," *IEEE J. Emerg. Sel. Topics Power Electron.*, vol. 1, no. 3, pp. 186–198, 2013.

[8] D. Rothmund, T. Guillod, D. Bortis, and J. W. Kolar, "99% Efficient 10 kV SiC-Based 7 kV/400 V DC Transformer for Future Data Centers," *IEEE J. Emerg. Sel. Topics Power Electron.*, vol. 7, no. 2, pp. 753–767, 2019.

[9] S. Falcones, R. Ayyanar, and X. Mao, "A dc-dc multiport-converter-based solid-state transformer integrating distributed generation and storage," *IEEE Trans. Power Electron.*, vol. 28, no. 5, pp. 2192–2203, 2013.

[10] Y. Yin, J. Wu, X. Zhou, L. Eeckhout, A. Qouneh, T. Li, and Z. Yu, "Copa: Highly cost-effective power back-up for green datacenters," *IEEE Trans. Parallel Dist. Syst.*, vol. 31, no. 4, pp. 967–980, 2020.

[11] D. Das and C. Kumar, "Partial startup scheme for smart transformer in meshed hybrid islanded grid operation," *IEEE Trans. Ind. Applicat.*, vol. 58, no. 1, pp. 142–151, 2022.

[12] A. Pouryekta, V. K. Ramachandaramurthy, N. Mithulananthan, and A. Arulampalam, "Islanding detection and enhancement of microgrid performance," *IEEE Syst. J.*, vol. 12, no. 4, pp. 3131–3141, 2018.

[13] W. Zheng, K. Ma, and X. Wang, "Hybrid energy storage with supercapacitor for cost-efficient data center power shaving and capping," *IEEE Trans. Parallel Distrib. Syst.*, vol. 28, no. 4, pp. 1105–1118, 2017.

[14] D. Das, H. V.M., and C. Kumar, "Bess-pv integrated islanded operation of st-based meshed hybrid microgrid," in *2020 IEEE 9th Int. Power Electron. Motion Control Conf. (IPEMC2020-ECCE Asia)*, 2020, pp. 2122–2128.

[15] H. V. M., C. Kumar, and M. Liserre, "An mvdc-based meshed hybrid microgrid enabled using smart transformers," *IEEE Trans. Ind. Electron.*, vol. 69, no. 4, pp. 3722–3731, 2022.

[16] C. Kumar and M. K. Mishra, "Operation and control of an improved performance interactive dstatcom," *IEEE Trans. Ind. Electron.*, vol. 62, no. 10, pp. 6024–6034, 2015.